

## Drop size spectra and integral remote sensing parameters in the transition from convective to stratiform rain

David Atlas<sup>1</sup> and Carlton Ulbrich<sup>2</sup>

Received 10 May 2006; revised 10 July 2006; accepted 17 July 2006; published 19 August 2006.

[1] Several authors have reported the correlation between the shape ( $\mu$ ) and slope ( $\Lambda$ ) of the gamma distribution of raindrops to reduce the number of parameters required to measure rainfall by remote sensing methods. However, we find that there are no well-defined  $\mu$ - $\Lambda$ , or associated relations between reflectivity ( $Z$ ) and rain rate ( $R$ ) or differential reflectivity for all storms or portions thereof. Rather, there is a general behavior such that  $A$  and  $b$  (in the  $Z = AR^b$  relation) and median volume drop diameter  $D_0$  all decrease from convective (C) to stratiform (S) to transition (T) rains. The  $\mu$ - $\Lambda$  correlation of the investigators in question appears to be limited to rainfall events which do not include convective rain; it is biased toward S and T rains. They miss the narrow (large  $\mu$ ), large  $D_0$  DSDs of convective rain that are often found to have equilibrium spectra. The dependence of  $D_0$  on the strength of the updraft and the findings of others concerning the association with the physics, dynamics, and climate regime strongly suggests that it is necessary to characterize the physical and dynamic nature of the storms in order to select the appropriate remote sensing algorithms. **Citation:** Atlas, D., and C. Ulbrich (2006), Drop size spectra and integral remote sensing parameters in the transition from convective to stratiform rain, *Geophys. Res. Lett.*, 33, L16803, doi:10.1029/2006GL026824.

### 1. Introduction

[2] Ulbrich [1983] has shown that the drop size distribution (DSD) is best represented by the gamma function

$$N(D) = N_0 D^\mu \exp(-\Lambda D) \quad (1)$$

where  $\mu$  is the shape parameter which increases as the breadth of the DSD decreases and  $\Lambda$  is the slope parameter which increases with the slope of the large size portion of the spectrum. (See Brangi and Chandrasekar [2001, p. 410] for the proper interpretation of  $N_0$ .) Because equation (1) contains three unknowns and present polarimetric and dual wavelength radar techniques can measure only two parameters, several authors have attempted to determine if there is a  $\mu$ - $\Lambda$  correlation. Such correlations have been reported by Zhang *et al.* [2001, hereinafter referred to as ZAL1, 2003, hereinafter referred to as ZAL2] and Brandes

*et al.* [2003, hereinafter referred to as BAL]. The latter report the relationship

$$\Lambda = 2.296 + 1.071\mu + 0.04325\mu^2 \quad (2)$$

The present work was motivated by our observations in the tropical oceanic rains of TOGA COARE [Atlas and Ulbrich, 2000, hereinafter referred to as AU; Atlas *et al.*, 1999, hereinafter referred to as AAL] which suggest that equation (2) is valid only for a very limited range of DSDs. Also observations from TRMM Large Scale Biosphere-Atmosphere Experiment (LBA) (Brazil) [Atlas and Williams, 2003], and Arecibo, PR [Ulbrich *et al.*, 1999] imply a greater variability of the  $\mu$ - $\Lambda$  relation than indicated by equation (2). However, the latter two geographic regions will be discussed in future work.

[3] Further detailed background on DSDs may be found in the work of Ulbrich [1983], Ulbrich and Atlas [1998], and others by the same authors which are extended and incorporated in the work by Rosenfeld and Ulbrich [2003] and Brangi and Chandrasekar [2001, section 7.1]. The latter book is a comprehensive treatment of the measurement of the properties of precipitation by polarimetric methods. Brangi *et al.* [2002] also present a methodology for estimating parameters of the gamma DSD from polarimetric measurements. Other relevant works are those of Sauvageot and Lacaux [1995] and Uijlenhoet *et al.* [2003]. Because the data used in the present paper have also been analyzed by AAL and AU we shall have frequent reference to the latter papers.

### 2. Drop Size Instrument

[4] All our drop size measurements were made with the Joss-Waldvogel Disdrometer (JWD [Joss and Waldvogel, 1967]; the JWD is also known as RD-69. The observations by ZAL1 and ZAL2 and BAL were made with a two dimensional video disdrometer [Kruger and Krajewski, 2002]. The pros and cons of the latter two instruments have been treated by a number of investigators. Tokay and Short [1996], Tokay *et al.* [2001], Williams *et al.* [2000], and Brangi *et al.* [2002] have discussed the limitations of the JWD with regard to both sample size and the masking of the small drops in the presence of larger ones. Sauvageot and Lacaux [1995] and AU have shown that the small drop masking effect by the JWD is not a limiting factor in most experiments. In particular we have conducted numerical experiments with various DSDs (not shown) which demonstrate that the larger moments of the DSD are only slightly changed by the masking affect at large rainfall rates.

[5] With regard to the drop sampling problem, some authors use two to five minute samples in order to minimize errors. Although we use one minute samples, the absence of

<sup>1</sup>Laboratory for Atmospheres, NASA Goddard Space Flight Center, Greenbelt, Maryland, USA.

<sup>2</sup>Department of Physics and Astronomy, Clemson University, Clemson, South Carolina, USA.

errors is easily shown by the lack of fluctuations of the median volume drop size ( $D_0$ ) in consecutive measurements (AU). It is only at the end of stratiform rain when the drop concentration and rain rates are very small that sampling errors become serious. On the other hand, truncation of the DSD by drop size sorting due to wind shear can be a critical problem for any point measurement either at the ground or aloft. The reader is also referred to *Zhang et al.* [2003] for a detailed study of the propagation of errors from DSD moment estimators to DSD parameters.

### 3. Observations

#### 3.1. The $\mu$ - $\Lambda$ - $D_0$ Relationship

[6] Figure 1 shows the  $\mu$ - $\Lambda$  observations taken on 17 January 1993 during TOGA COARE (TC) as reported by AAL and AU (see their Figure 2 and Table 2). The smooth curve corresponds to equation (2) of BAL. The lines of constant  $D_0$  were derived on the basis of  $D_0 = (3.67 + \mu)/\Lambda$  as shown by *Ulbrich and Atlas* [1998] for a gamma DSD. Although the relationship between the three parameters in Figure 1 has been well known since *Ulbrich* [1983], this is evidently the first time that it has been shown explicitly to permit the comparison of observations to theory. A color code is used to indicate the stage of storm development, viz., red for convective (C), green for transition (T), and blue for stratiform (S). The shape of the symbols corresponds to the ranges of  $D_0$  shown in the legend at the lower right. Such a five-parameter display provides both quantitative data and insights concerning the responsible physical processes. The properties of all the samples were obtained by the method of moments [*Ulbrich and Atlas*, 1998].

[7] The following features in Figure 1 are apparent. First, the circular red dots, corresponding to the 24 minute convective region, tend to have the largest values of  $D_0$  and  $\mu$  and fall close to the theoretical  $D_0 = 2.0$  mm isopleth. The values of  $\mu$  ranging from 6 to 15 are associated with narrow DSDs. Moreover, the associated values of  $\Lambda$  do not exceed  $10.5 \text{ mm}^{-1}$ . Such features of narrow spectra of large drops have long been known to correspond to the initial rains from convective clouds.

[8] Second, with few exceptions the green squares associated with the transition (T) rainfall occur near the  $D_0 = 1$  mm contour, and exhibit a broad range of  $\mu$  and  $\Lambda$  while the stratiform (S) blue squares tend to fall close to the  $D_0 \approx 1.5$  mm intermediate to the those in the C and T periods. The latter points also exhibit a broad range of  $\Lambda$ . This kind of behavior is manifested by the fairly systematic variation of the coefficient A and exponent b in the radar reflectivity-rain rate relationship  $Z = AR^b$ , as shown by AAL (their Figure 9) where A decreases and b increases from C to S to T rainfall. A similar variation is also suggested less dramatically in the early work of *Fujiwara* [1965] (shown better by *Kodaira and Aoyagi* [1990]).

[9] Finally, the constrained gamma curve of BAL falls between  $1 < D_0 < 1.5$  mm except at the largest  $\Lambda$ . It is therefore clear that the BAL  $\mu$ - $\Lambda$  relation was dominated by small  $D_0$  values associated with either S or T rains. The primary difference between the present observations and those of BAL, ZAL1 and ZAL2 is the large drop sizes ( $D_0$ ) and narrow distributions (large  $\mu$ ) associated with the initial convective rain. Furthermore, it is particularly interesting

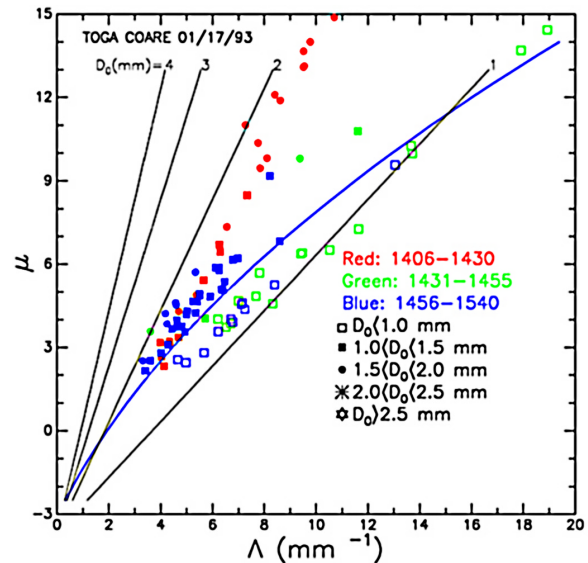


**Figure 1.** Plot of the gamma DSD parameter  $\mu$  versus  $\Lambda$  for a thunderstorm observed on 17 January 1993 during TOGA COARE. The red, green and blue points correspond to observations acquired during the convective, transition and stratiform portions of the storm, respectively. The different symbols used correspond to ranges of median volume diameter,  $D_0$ , as in the legend. The straight lines labeled with values of  $D_0$  correspond to the theoretical relation  $\Lambda D_0 = 3.67 + \mu$ . The curve corresponds to the relation of equation (2) after *Brandes et al.* [2003].

that the  $D_0$  values in the convective rain are nearly constant (between 1.73 to 1.99 mm). This can also be seen in the time trace of  $D_0$ , R, and Z in AAL (Figure 1). In other words this convective rain is comprised of essentially equilibrium DSDs in which all the moments and  $D_0$  are constant while the rain rate varies only with the drop number concentration. Corresponding features of the  $Z = AR^b$  relationship are that b approaches unity [*List*, 1988; AU] while A increases with  $D_0$ . The absence of such values of b in the literature [*Rosenfeld and Ulbrich*, 2003] is probably due to the failure to divide the observations into C, T, and R rains.

[10] Although no such large  $D_0$  values are possible in the  $\mu$ - $\Lambda$  relations of BAL, ZAL1 or ZAL2 based upon observations in Oklahoma and Florida, respectively, *Zhang et al.* [2006] show a plot of differential radar reflectivity ( $Z_{dr}$ ) which correspond to  $2.0 < D_0 < 2.5$  mm in Florida convective rains. The discrepancy between the latter results and their earlier ones is unexplained by the authors.

[11] Clearly, it is important to get the Z-R relation for convective rain as accurately as possible because it is this rain that often accounts for the lion's share of the total storm rainfall. In the storm of Feb 17, 1993 the 24 min convective rain accounted for 67% of the 94 min accumulation. We shall return to the nature of the physical processes responsible for equilibrium DSDs later.

#### 3.2. $Z_{dr}$ - $D_0$ -Z Relationship

[12] In order to determine the relationship between the differential reflectivity at horizontal (H) and vertical (V) polarization  $Z_{dr}$  and the total Z at H polarization we first use the relationship of *Bringi and Chandrasekar* [2001],  $D_0 = 1.53 (Z_{dr})^{0.467}$ . Figure 2 is a plot of the experimental values

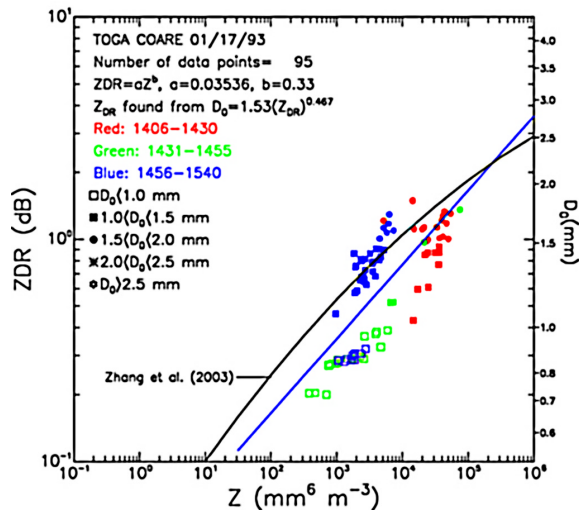


**Figure 2.** Plot of differential reflectivity,  $Z_{dr}$ , versus reflectivity factor,  $Z$ , for the same data as shown in Figure 1. The plotting conventions are the same as in Figure 1. The curved line that passes mostly through the blue points is the empirical relation of *Zhang et al.* [2003]. The straight blue line is an empirical fit to the data of a relation of the form  $Z_{dr} = aZ^b$ , where the values of  $a$  and  $b$  are shown in the figure.

of differential reflectivity  $Z_{dr}$  (left axis) and  $D_0$  (right axis) vs  $Z$  for the same data shown in Figure 1. The smooth curve is from *Zhang et al.* [2003] in accord with the constrained gamma DSD. The straight line is the regression relation in the legend. The separation of the C (red), T (green), and S (blue) points is clear. While the range of  $Z_{dr}$  and  $D_0$  is similar for both the C and S rain, the  $Z$  values for the convective rains are an order of magnitude larger and the points fall well below the ZAL relation.

[13] Figure 3 presents a plot similar to that in Figure 2 for 26 Jan 1993 in TOGA COARE. The separation of C, T, and S data is again pronounced. Here the largest  $Z_{dr}$  and  $D_0$  values occur in the second segment of “stratiform” rain with  $D_0 \approx 2.3$  mm, while the C rain (red) has the largest  $Z \approx 51$  dBZ. Now, virtually all of the data points for all the rain types fall either above or below the ZAL curve. Neither is our regression relationship (see legend) a good representation of the data. As on Feb 17 the T rain has the smallest  $D_0$  values and correspondingly small  $Z_{dr}$ . Also, the asymptotic value of the data is  $D_0 \approx 2$  mm and  $Z \approx 50$  dBZ.

[14] Reference to Plate 1 of AAL shows that the second period of stratiform rain, of 70 min duration, occurs under an unusually strong Bright Band. The latter rain appeared below a precipitation streamer with a top near 12 km; it is evidently the fallout from the anvil ejected from the convective turret upstream. This period is marked by the very large and nearly constant  $D_0$  values (shown by the crosses in Figure 3) with  $Z = 865R^{1.08}$  (AAL, Table 1). It thus corresponds to an apparent equilibrium DSD. However, during this period Plate 1 of AAL shows that  $Z$  and mean Doppler fall speed both decrease downward below the melting level. Such a combination suggests evaporation of the smaller drops, thus leaving the larger drops to dominate. Another alternative is drop breakup of giant drops. Apparently, drop size sorting by wind shear is also at play to

truncate the smaller drops observed by the JWD. The TOGA COARE soundings for this date support this interpretation. In short, one must exert care in the interpretation of point observations at the ground.

#### 4. Physical Processes

[15] The physical mechanisms responsible for the variety of Z-R relations have been treated well by *Rosenfeld and Ulbrich* [2003]. Here we are concerned only with the development of equilibrium DSDs that occur often in the convective portions of intense storms regardless of their geographical location [*List*, 1988; *Hu and Srivastava*, 1995]. In essence, the combination of a high  $0^\circ\text{C}$  level, large moisture content, and strong updrafts in continental tropical storms permits the collision-coalescence-breakup (CCB) process to dominate the formation of the DSD below regardless of the nature of the microphysical processes above the  $0^\circ\text{C}$  level. In other words, given sufficient time to operate the CCB mechanism will lead to equilibrium DSDs.

[16] In the case of warm oceanic rainfall with weaker updrafts and lower  $0^\circ\text{C}$  levels, the essential elements of the process leading to equilibrium are: 1) the growth of droplets by collision and coalescence over an extended period due to the support of medium size drops; 2) the sorting of drop sizes such that the smaller ones are carried aloft where they are evacuated in the divergent flow above the updraft maximum, and the descent of the larger fast falling drops to the surface in a relatively narrow distribution with large  $D_0$ . In other words larger drops and  $D_0$  are determined by the strength of the updraft. Refer to AU for a more detailed description and supporting experimental evidence for the occurrence of equilibrium DSDs in the warm tropical oceanic environment.

[17] In view of the giant drops of 8 mm diameter and reflectivity of 60 dBZ observed in warm convective rain with updrafts of only 5 to 9  $\text{m s}^{-1}$  off the NE coast of Hawaii [*Szumowski et al.*, 1997], one may also suggest that an equilibrium DSD may sometimes result from the breakup of larger drops.

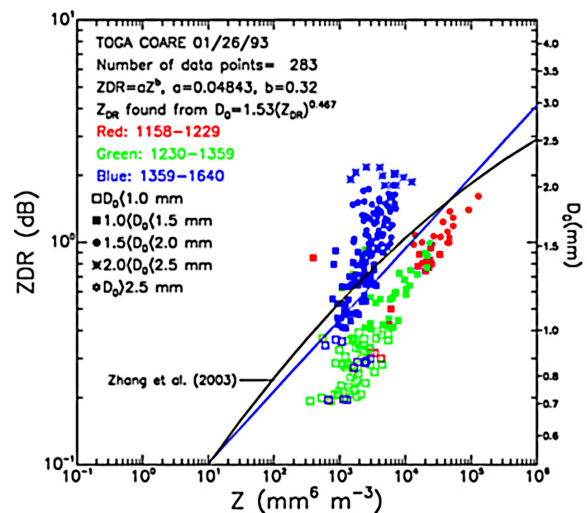


**Figure 3.** Same as Figure 2 except for the TOGA COARE storm on 26 January 1993.

[18] Even in the more vigorous updrafts in continental tropical rains found in Rondonia, Brazil during TRMM-LBA, one finds equilibrium DSDs which have formed predominantly in the warm layers below the freezing level while melt water rainfall is entering that zone from above [Atlas and Williams, 2003]. Similar preliminary results have been found using data for other thunderstorms from Arecibo, Puerto Rico [Ulbrich *et al.*, 1999]. The freezing levels in both Brazil and Puerto Rico are higher than those in the tropical oceanic Pacific. While the precipitation may occur from graupel, hail, and snow aloft, it is the CCB process which controls the DSDs near the surface as noted above and demonstrated in the model results of Hu and Srivastava [1995]. The rain thus reaches broader (smaller  $\mu$ ) equilibrium DSDs than those found in oceanic rainfall. Also, the  $D_0$  and  $Z$  values are close to the largest found with asymptotic values of  $D_0 \approx 3$  mm and  $Z = 53$  dBZ as also shown by Bringi *et al.* [2002]. This is consistent with the expectation that  $D_0$  increases with the updraft speed.

[19] It is also of interest that Bringi *et al.* [2003] have recently used analysis of polarimetric radar and disdrometer data to formulate a method of classification of rainfall types. They use the mass-weighted mean diameter  $D_m$  and the parameter  $N_w$  which is the normalized intercept parameter of an equivalent exponential DSD that has the same water content and median volume diameter ( $D_0$ ) as the gamma DSD. The latter parameter is proportional to the liquid water concentration  $W$  and inversely proportional to the fourth power of  $D_m$ . On plots of  $N_w$  versus  $D_m$  they find a pronounced separation of relations for S and C rainfall. They also find maritime-like and continental-like “clusters” on the  $N_w - D_m$  plane for convective rain that appear to be related to the coefficient A in  $Z = AR^b$  relations.

[20] A similar classification scheme was also devised by Rosenfeld and Ulbrich [2002]. It was accomplished through examination of integral parameters deduced from the DSD associated with the host of  $Z$ - $R$  relations found in the literature. The latter parameters are deduced from the coefficient and exponent of empirical  $Z$ - $R$  relations using a gamma DSD. They used the liquid water concentration  $W$  and  $D_0$ . A physically based classification of the DSDs shows remarkable ordering of the  $W$  versus  $D_0$  relations, which provides insight to the fundamental causes of the organized differences in  $Z$ - $R$  relations. Emphasis was placed on cloud microstructure between “continental” and “maritime”, and cloud dynamics between “convective” and “stratiform.” The latter classification scheme explains large systematic variations in  $Z$ - $R$  relations between maritime and continental clouds, stratiform and maritime convective clouds, and orographic precipitation. The scheme reveals the potential for significant improvements in radar rainfall estimates by application of a dynamic  $Z$ - $R$  relation, based on the microphysical, dynamical and topographical context of the precipitation. This is the direction which Bringi *et al.* [2003] have also taken and the one that we advocate in the present work.

## 5. Conclusions

[21] From the above it is clear that there are no well defined  $\mu$ - $\Lambda$ ,  $Z$ - $R$  or  $Z_{dr}$ - $Z$  relations for all storms or portions thereof. However, there is a general behavior such that  $D_0$ ,

A, and b (in the  $Z = AR^b$  relation) all decrease from convective (C) to stratiform (S) to transition (T) rains. The  $\mu$ - $\Lambda$  correlation of Zhang *et al.* [2003] and Brandes *et al.* [2003] appears to be limited to rainfall events which do not include convective rain; it is biased toward S and T rains. They miss the narrow (large  $\mu$ ), large  $D_0$  DSDs of convective rain. Nor can such a relation be used for parameterization in microphysical models.

[22] The fairly regular occurrence of equilibrium DSDs with large  $D_0$  in the initial convective rain focuses attention on the physical processes involved. This is due mainly to the extended period of warm growth by collision, coalescence and breakup (CCB) to large sizes when suspended in an updraft, and the sorting of the drops by the updraft speed. The dependence of the magnitude of  $D_0$  on the updraft, and the findings by others, strongly suggests that it is necessary to characterize the physical and dynamic nature of the storms in order to select the appropriate remote sensing algorithms.

[23] **Acknowledgments.** Although this work was conducted without any institutional support we are both grateful to our institutions for the continued hospitality that they have extended to us. Since this work is an extension of that which we have done over the last 34 years we also express appreciation to all of our colleagues at NCAR, NASA, and NOAA and a number of universities who have collaborated with and stimulated us.

## References

- Atlas, D., and C. W. Ulbrich (2000), An observationally based conceptual model of warm oceanic convective rain in the tropics, *J. Appl. Meteorol.*, **39**, 2165–2181.
- Atlas, D., and C. R. Williams (2003), The anatomy of a continental tropical convective storm, *J. Atmos. Sci.*, **60**, 3–15.
- Atlas, D., C. W. Ulbrich, F. D. Marks, E. Amitai, and C. R. Williams (1999), Systematic variation of drop size and radar-rainfall relations, *J. Geophys. Res.*, **104**, 6155–6169.
- Brandes, E. A., G. Zhang, and J. Vivekanandan (2003), An evaluation of a drop-distribution based polarimetric radar rainfall estimator, *J. Appl. Meteorol.*, **42**, 652–660.
- Bringi, V. N., and V. Chandrasekar (2001), *Polarimetric Doppler Weather Radar: Principles and Applications*, 636 pp., Cambridge Univ. Press, New York.
- Bringi, V. N., G.-J. Huang, and V. Chandrasekar (2002), A methodology for estimating the parameters of a gamma raindrop size distribution model from polarimetric radar data: Application to a squall-line event from the TRMM/Brazil campaign, *J. Atmos. Oceanic Technol.*, **19**, 633–645.
- Bringi, V. N., V. Chandrasekar, J. Hubbert, E. Gorgucci, W. L. Randeu, and M. Schoenhuber (2003), Raindrop size distribution in different climatic regimes from disdrometer and dual-polarized radar analysis, *J. Atmos. Sci.*, **60**, 354–365.
- Fujiwara, M. (1965), Raindrop-size distribution from individual storms, *J. Atmos. Sci.*, **22**, 585–591.
- Hu, R. C., and R. C. Srivastava (1995), Evolution of raindrop size distributions by coalescence, breakup, and evaporation: Theory and observation, *J. Atmos. Sci.*, **52**, 1761–1783.
- Joss, J., and A. Waldvogel (1967), Ein Spektrograph für Niederschlagestropfen mit automatischer Auswertung, *Pure Appl. Geophys.*, **68**, 240–246.
- Kodaira, N., and J. Aoyagi (1990), History of radar meteorology in Japan, in *Radar in Meteorology*, edited by D. Atlas, pp. 69–76, Am. Meteorol. Soc., Boston, Mass.
- Kruger, A., and W. F. Krajewski (2002), Two-dimensional video disdrometer: A description, *J. Atmos. Oceanic Technol.*, **19**, 602–617.
- List, R. (1988), A linear radar reflectivity-rainrate relationship for steady tropical rain, *J. Atmos. Sci.*, **45**, 3564–3572.
- Rosenfeld, D., and C. W. Ulbrich (2003), Cloud microphysical properties, processes, and rainfall estimation opportunities, *Meteorol. Monogr.*, **30**, 237–258.
- Sauvageot, H., and J.-P. Lacaux (1995), The shape of averaged drop size distributions, *J. Atmos. Sci.*, **52**, 1070–1083.
- Szumowski, M. J., R. M. Rauber, H. T. Ochs, and L. J. Miller (1997), The microphysical structure and evolution of Hawaiian rainband clouds. Part I: Radar observations of rainbands containing high reflectivity cores, *J. Atmos. Sci.*, **54**, 369–385.

- Tokay, A., and D. A. Short (1996), Evidence from tropical raindrop spectra of the origin of rain from stratiform and convective clouds, *J. Appl. Meteorol.*, *35*, 355–371.
- Tokay, A., A. J. Kruger, and W. F. Krajewski (2001), Comparison of drop size distribution measurements by impact and optical disdrometers, *J. Appl. Meteorol.*, *40*, 2083–2097.
- Uijlenhoet, J., A. Smith, and M. Steiner (2003), Variability of raindrop size distributions in a squall line and implications for radar rainfall estimation, *J. Atmos. Sci.*, *60*, 1220–1238.
- Ulbrich, C. W. (1983), Natural variations in the analytical form of the raindrop size distribution, *J. Appl. Meteorol.*, *22*, 1764–1775.
- Ulbrich, C. W., and D. Atlas (1998), Rainfall microphysics and radar properties: Analysis methods for drop size spectra, *J. Appl. Meteorol.*, *37*, 912–923.
- Ulbrich, C. W., M. Petitdidier, and E. F. Campos (1999), Radar properties of tropical rain found from disdrometer data at Arecibo, PR, paper presented at 28th Conference on Radar Meteorology, Am. Meteorol. Soc., Montreal, Quebec, Canada.
- Williams, C. R., A. Kruger, K. S. Gage, A. Tokay, R. Cifelli, W. F. Krajewski, and C. Kummerow (2000), Comparison of simultaneous raindrop size distributions estimated from two surface disdrometers and a UHF profiler, *Geophys. Res. Lett.*, *27*, 1763–1766.
- Zhang, G., J. Vivekanandan, and E. Brandes (2001), A method for estimating rain rate and drop size distribution from polarimetric radar measurements, *IEEE Trans. Geosci. Remote Sens.*, *39*, 830–841.
- Zhang, G., J. Vivekanandan, and E. A. Brandes (2003), The shape–slope relation in observed gamma raindrop size distributions: Statistical error or useful information?, *J. Atmos. Oceanic Technol.*, *20*, 1106–1119.
- Zhang, G., J. Sun, and E. A. Brandes (2006), Improving parameterization of rain microphysics with disdrometer and radar observations, *J. Atmos. Sci.*, *63*, 1273–1290.
- 
- D. Atlas, Laboratory for Atmospheres, Code 613, NASA Goddard Space Flight Center, Greenbelt, MD 20771, USA. (davnl@comcast.net)
- C. Ulbrich, Department of Physics and Astronomy, Clemson University, 106 Highland Drive, Clemson, SC 29634, USA.